SEMICONDUCTOR–INSULATOR–SEMICONDUCTOR STRUCTURES

Semiconductor–insulator–semiconductor wafers consist of three layers: a crystalline semiconductor top layer, an amorphous insulator middle layer, and a semiconductor substrate

at the bottom, which constitutes the rest of the wafer. Most uses require submicron top and middle layers, although there are niche markets for thicker layers. The top semiconductor layer acts as a "substrate" for electronic devices, and the buried oxide underneath provides a convenient way to isolate adjacent devices. First introduced more than 25 years ago, these structures were designed to minimize damage caused by sudden pulses of ionizing radiation. For example, semiconductor-insulator-semiconductor wafers eliminate "latch up," the unintentional conduction between devices closely spaced on a standard silicon substrate. More recently, the low voltage operation and minimized capacitance made possible with these three layered structures have attracted the attention of the low power electronics industry. Here we concentrate on the materials and electrical issues involved in fabrication and use.

Although several combinations of semiconductor and insulator materials are being investigated, the most fully developed is the silicon-silicon dioxide-silicon structure. For this reason, we concentrate solely on the silicon/oxide system, which is generically referred to as silicon on insulator (SOI). Figure 1 shows a schematic of the three layered wafer. The oxide between the two layers of silicon is referred to as the buried oxide (BOX). The two most common methods today for fabricating an SOI wafer are separation of silicon by the implantation of oxygen (SIMOX) and bonded silicon on insulator (BSOI). The general fabrication techniques along with several variations are outlined in what follows. Two other fabrication processes, zone melt recrystallization (ZMR) and lateral overgrowth, are not strong competitors for the SOI market. The reader is referred to Ref. 1 for more information on these techniques.

FABRICATION AND MATERIALS ISSUES

Separation of Silicon by Implantation of Oxygen

In the late 1970s, Anand and Badawi (2) proposed that an SiO_2 layer formed by high dose oxygen implantation into crystalline Si and subsequent annealing would make a suitable substrate for microelectronics. The typical formation procedure for SIMOX consists of implanting 180 keV oxygen ions into Si to a dose of $1.8 \times 10^{18}/cm^{-2}$ while the Si substrate is held at 500 or 600°C. The implanted wafer is annealed at about 1325°C for 5 or 6 h in an Ar + 1% O_2 ambient. The procedure produces a 400 nm amorphous SiO_2 layer below about 200 nm of crystalline Si, and will be referred to hereafter as standard SIMOX. Typical cross-sectional transmission electron microscopy (XTEM) micrographs reveal three layers
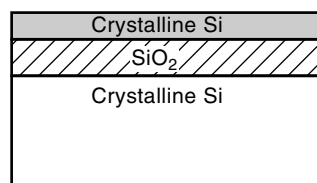
of high-quality material separated by well-defined boundaries.

Despite the initial success of the standard SIMOX wafers, subtle deficiencies have prompted the introduction of several processing variations. For example, in one modification, the oxygen is implanted in stages, each of which consists of roughly one-half or one-third of the total dose (3). After each implant step, the material is cleaned and given an anneal at 1325°C for 5 h. The implant/anneal process is repeated until the full dose is implanted. The resulting material is called double or triple implant SIMOX, depending on whether two or three stages are used. Another variation involves introducing additional oxygen into the buried layer by implanting a small dose of O after the standard SIMOX process. Typically, about 10% of the original amount is implanted into the buried oxide, and the structure is annealed at 1000°C for 1 h in Ar + 1% O_2. Although this "supplemental implantation" process compensates for the inherent oxygen deficiency and improves electrical response, the straggle from the implant beam produces excess O in the Si layer (see the section in this article entitled "Electron Paramagnetic Resonance"). Low power applications and a drive to decrease production costs have prompted one of the most recent variations for SIMOX fabrication, the use of a smaller total dose (4). One process utilizes 0.4×10^{18} cm^{-2} rather than 1.8×10^{18} O cm^{-2} to produce a 300 nm Si layer and 80 nm buried oxide (5). As discussed in the section entitled "Electrical Characterization" leakage through the thinner oxide is a major problem, but recent experimentation with post-fabrication oxidation minimizes this effect. The additional oxidation, referred to as internal thermal oxidation (ITOX) involves exposing the SIMOX wafer to O_2 at 1325°C (5,6). Others have formed a thin buried oxide by augmenting the standard low dose SIMOX process with an additional "touch" of implanted oxygen (1×10^{15} cm^{-2}) while the substrate temperature is maintained close to room temperature (7). The relatively new techniques remain to be fully assessed.

Bonded Silicon on Insulator

Bonded SOI involves an Si oxidation step, a bonding procedure, and a thinning process (8,9). One or two wafers is oxidized. The "handle" wafer becomes the substrate and the "seed" wafer provides the thin top Si layer. An oxide is thermally grown on the handle and/or seed wafers. If the wafers are placed in contact with each other at room temperature, weak hydrogen bonds form between them. The bond is strengthened by heating the wafers at temperatures greater than 800°C in N_2 or O_2. Typically, a temperature between 900° to 1100°C and a time of 1 to 2 h produces a satisfactory bond. The bulk of the Si seed wafer is removed by one of two methods depending on the desired thickness of the remaining top Si layer. For thicknesses greater than 1 μm, a combination of grinding and polishing is used. For a thinner top Si layer, an etch stop is formed in the seed wafer prior to oxidation, and a combination of grinding and chemical etching is used to remove the Si. This latter process is the one referred to as bond and etch-back SOI (BESOI). The first successful demonstration of this technique is attributed to Lasky (see Ref. 8).

Several different types of chemical and plasma techniques have already been employed to etch the Si wafer to the desired thickness but a new method to remove the Si substrate

Figure 1. Schematic diagram of SOI structure. The thicknesses of the top silicon layer and buried SiO_2 layer depend on the fabrication process and vary from 100 nm to 1 μm. The substrate is typically about 0.5 mm thick.

and form the top Si layer was introduced recently (10). A dose of 10^{16} cm^{-2} to 10^{17} cm^{-2} hydrogen ions are implanted into the oxidized seed wafer. The depth of the implant below the Si surface coincides with the thickness of the final top silicon layer. After bonding, the structure is thermally treated at 400° to 600°C. The implanted layer serves as a perforation that breaks during this thermal cycle. The silicon substrate literally pops off the bonded wafer and leaves a thin top silicon layer. After the final annealing and polishing, a clean, thin, uniform top Si layer is achieved. This new method, referred to as Unibond using the Smart Cut procedure, circumvents the difficulties encountered with etch stops and eliminates loss of an entire Si wafer. This new technique achieves good thickness uniformity of the silicon and oxide layers and the substrate that pops off from the bonded wafers may be recycled for another bonded SOI wafer. Side effects related to the hydrogen introduced during the process have not yet been fully addressed.

SIMOX Formation

Because the formation of a SiO$_2$ layer by implantation of oxygen into silicon is very different from the thermal oxidation process employed for BSOI technology, we expand somewhat on the formation process. Nakashima and Izumi have done an extensive study of the buried oxide formation in SIMOX (11,12). Using XTEM, they have examined oxygen implanted at 180 keV at 550°C over a dose range from 0.1 to 2.0 × 10^{18}/cm^2. One compelling feature of their study is the broad dose range and the finely stepped gradations used. For each dose, the evolution of the oxygen was examined as the annealing temperature ranged from 1050° to 1350°C. Although higher than the standard device processing temperature, this temperature range is necessary to repair the damage in the top Si layer. Presumably, the high melting point of Si (1415°C) necessitates the high annealing temperatures. The work of Nakashima and Izumi (11,12) demonstrated the complicated interplay between the oxygen dose, annealing temperature and macroscopic defects in the final annealed material.

Before annealing, there is redistribution of oxygen during the implantation. The peak in the local oxygen concentration reaches the stoichiometry of SiO$_2$ at a dose of 1.2 × 10^{18}/cm^2. At higher doses, this stoichiometry is not exceeded. Oxygen migrates from the peak of the implantation range profile to the tails of the profile leaving a flat-topped distribution of oxygen. More oxygen diffuses toward the top silicon layer because of the higher implantation damage nearer the wafer surface. Thus, for doses of 1.2 × 10^{18}/cm^2 and above, a stoichiometric buried oxide layer is formed during implantation. Oxygen atoms are also locally redistributed in regions in which the oxygen concentration is lower. This includes the whole implanted region for doses below 1.2 × 10^{18}/cm^2 and the tails of the distribution for higher dose implants. There is a partial phase separation into interspersed areas of high and low oxygen concentration. No threading dislocations are observed after implantation.

As the annealing temperature is increased from 1050° to 1350°C, oxygen segregation increases. There is preferential growth of large oxygen precipitates as smaller precipitates are dissolved. For doses of 1.2 × 10^{18}/cm^2 and above, the oxygen precipitates coalesce and are eventually absorbed into the buried oxide layer. Near the oxide-silicon interfaces, as the oxygen segregates, layers of silicon and oxygen precipitates can form. As these layers coalesce into the buried oxide, silicon islands within the buried oxide are formed. When present, these islands are clearly visible in the XTEM micrographs and have the same crystallographic orientation as the silicon wafer. After the 1350°C anneal, a top silicon layer that is free of oxygen precipitates is formed. The interfaces between the buried oxide and the silicon layers above and below it are smooth and atomically abrupt. If present, the silicon islands are not removed by annealing at 1350°C. The number of silicon islands tends to decrease as the dose increases. In contrast, the number of dislocations increases with increasing dose.

For doses below 1.2 × 10^{18}/cm^2, the initial annealing is characterized by the growth of oxygen precipitates that tend to form alternating oxide and silicon layers near the peak of the oxygen implant. As larger oxygen precipitates grow and smaller ones are dissolved, these layers coalesce into a buried oxide. As the precipitates are absorbed into the buried oxide, dislocations between the precipitates are eliminated. For doses between 0.4 and 1.2 × 10^{18}/cm^2 the dislocation density is very low, <10^3/cm^2. In the dose range from 0.5 to 1.2 × 10^{18}/cm^2 a high concentration of silicon islands remains in the oxide after annealing at 1350°C. In the dose range of 0.35 to 0.4 × 10^{18}/cm^2 Nakashima and Izumi (11,12) found that SIMOX with low dislocation density and no silicon islands could be formed. The lack of islands produced an oxide with a high breakdown voltage. At still lower doses the buried oxide was not continuous, thereby leading to a high dislocation density.

To compete with standard silicon the top silicon layer of a SOI wafer must be as defect-free as bulk Si, and the buried oxide must not introduce deleterious complications such as leakage current or charge imbalance. Both BSOI and SIMOX technologies strive continuously to meet these criteria. The remainder of the article addresses SOI quality at three different levels. The first part focuses on extended defects observed by techniques such as electron microscopy and chemical etching. Then, in the section on electrical characterization, the electrical response of the SOI wafers is reported. The article closes with a description of the structure and charge state of point defects identified by electron paramagnetic resonance (EPR). A summary at the end highlights the challenges facing the future of silicon-insulator-silicon structures.

EXTENDED DEFECTS

At the microscopy level, considerably different problems afflict SIMOX and BSOI material. Therefore, each will be treated separately in this section.

Metallic contamination (e.g., Fe, Ni, and Cu) was a serious problem in early SIMOX material. Because most of the impurities came from the implanters and high-temperature annealing furnaces, thorough cleaning has reduced significantly the type and density of metal impurities. The newest implanters specifically designed for fabricating SIMOX have reduced metal contamination appreciably. Also, multiple implantation appears to have minimized the introduction of metallic particles. Today, metal contamination in SIMOX is approximately the same as in silicon.

The density of dislocations and stacking faults can vary greatly in the different types of SIMOX wafers. A stacking fault results from the displacement of a plane of atoms and a dislocation represents a misplaced column or row of atoms. Stoemenos reports that standard SIMOX contains on the order of 10^6 cm^{-2} dislocations and stacking faults (3). The density of both is reduced to 10^4 cm^{-2} by the multiple implantation process. Low-dose and/or low-energy implantation can also reduce the density of dislocation and stacking faults. For example, Nakashima and Izumi show that 2×10^{18} cm^{-2} dose yields material with a dislocation density of 1×10^9 cm^{-2}; a dose of 0.35–1.2×10^{18} cm^{-2} O can lower the number to 1×10^3 cm^{-2} (12).

Another problem that plagues SIMOX wafers is the presence of excess Si in the buried oxide and oxygen interstitials in the Si layers. Nakashima shows that Si precipitates appear in material fabricated using doses greater than 0.7×10^{18} O cm^{-2} (12). In standard SIMOX, these precipitates coalesce into 5 nm to 100 nm long "islands" occupying about 2% of the buried oxide (3). The Si islands appear in the oxide near the substrate/buried oxide interface. Multiple implantation reduces their density to about 0.5% (3). Supplemental SIMOX and ITOX are also successful at minimizing the Si concentration in the buried layer.

The concentration of oxide precipitates in the silicon is reduced greatly by the high-temperature SIMOX anneal; however, both electron microscopy micrographs and EPR spectra indicate that some precipitates exist in SIMOX. The concentration tends to be higher in low-dose material (less than 1.2×10^{18} cm^{-2} O implanted) than in standard SIMOX (O dose equal 1.8×10^{18} cm^{-2}) (12). Ironically, the presence of the oxide precipitates during the high-temperature anneal is thought to minimize the formation of threading dislocations during the anneal. Careful processing, however, can minimize both.

Although BSOI wafers contain about the same level of metallic impurities as found in SIMOX, extended defects are not a serious concern in bonded material. Two major problems afflict BSOI wafers: voids and etch pits (8,9). The first is responsible for weak or incomplete bonding. The voids, which vary in size from a few mm^2 to a few cm^2, form from particulates or gaseous species trapped between the wafers during the bonding process and/or during subsequent annealing. Extremely careful preparation and handling of the oxidized wafers minimizes the void formation. Etch pits are thought to be created during the implantation of the etch stop layer or during deposition of an epitaxial Si layer employed in some of the chemical etching processes. Densities ranging from 300 cm^{-2} to 1000 cm^{-2} have been reported (9).

A common feature of BSOI and SIMOX processing is the high-temperature annealing step (as high as 1350°C for SIMOX and 1100°C for BSOI) that follows buried oxide formation. Beyond the techniques already described here, both spectroscopic and electrical characterization reveals deterioration of the buried oxide layer after high-temperature annealing. Specific results pertaining to electrical measurements and EPR will be discussed in detail in the following two sections, but two notable results not included there should be mentioned. During the high-temperature anneal, infrared spectroscopy indicates an increase in the 1106 cm^{-1} absorption, which is ascribed to O interstitials in Si (13). The study suggests that oxygen leaves the BOX during the high-temperature anneal, a result consistent with the appearance of excess Si in the buried layer. The same investigation reports atomic force microscopy (AFM) data which show that the buried oxide and oxide/substrate interface are roughened by the high-temperature annealing step. Both sets of results were obtained on Si–SiO$_2$–Si structures formed by polysilicon deposition on a thermal oxide, but there is every reason to believe a comparable process occurs in technological structures such as SIMOX or BSOI. Indeed, similar conclusions concerning O migration from the buried oxides were derived by others performing secondary ion mass spectroscopy on SIMOX samples (14).

The uniformity and roughness of the top Si layer is a major issue for all SOI fabrication techniques. Recent reports show surfaces with a uniformity of about 10 nm over a 200 mm wafer. With sufficient polishing, surface roughness of BSOI wafers (0.05 nm to 0.1 nm) rivals Si (0.05 to 0.08), while the surface roughness of SIMOX, which receives no final polishing, is higher (0.25 nm to 0.45 nm) (4). (Numbers are from analysis of 200 nm BOX SOI.) Both surface roughness and uniformity approach the levels of a bulk Si wafer.

In summary, the major extended defects affecting Si–SiO$_2$–Si structures are excess Si in the buried oxide of SIMOX and the presence of voids at the bonded interface of BSOI. One method that alleviates the excess Si problem in SIMOX is the supplemental O implantation process. Investigators are pursuing a variety of annealing and cleaning processes to address the issue of bonding in BSOI. Despite these remaining difficulties, both SIMOX and BSOI wafers are standard products used for radiation hard and high voltage devices. Processing adaptations designed for new markets, such as forming thin BOX in SIMOX for low-power applications, provide evidence of the continuing interest in the SOI.

ELECTRICAL CHARACTERIZATION

Excess Oxide Conduction in SIMOX

The unconventional method by which the buried oxide layer is formed in SIMOX wafers has led to problems with conduction through the buried oxide layer. Two types of conduction problems, both due to excess silicon in the buried oxide, have been observed. The first is due to macroscopic inclusions of silicon within the buried oxide that cause localized shorts or low-voltage breakdown. Brown and Revesz have discussed silicon "pipes" within the oxide (15). Low-voltage shorts were attributed to inclusions that spanned the oxide. Inclusions that partially cross the oxide introduce oxide breakdown locations and decrease the breakdown voltage. One source of silicon pipes spanning the oxide is particulate contamination. Particles on the wafer can mask the oxygen implant sufficiently to leave a silicon column through the buried oxide (16). As discussed in the previous section, silicon inclusions can also be formed during the buried oxide formation process.

The second type of conduction is not localized but scales with the area (17). In fields up to 2 MV/cm to 3 MV/cm the current is quasi-ohmic and decreases with time. At higher fields, the current increases exponentially. The temperature dependence of the conduction is weak. Revesz et al. examined the conduction between 25° and 300°C, and Stahlbush et al. measured from 40 K to 300 K (27°C) (17,18). The temperature dependence eliminates Poole-Frenkel or Schottky conduction

mechanisms. Both groups concluded that the conduction is very similar to the behavior of silicon-rich oxides deposited by chemical vapor deposition (CVD) techniques (19). The silicon-rich CVD oxides were shown to consist of a two-phase mixture of silicon clusters 1 nm to 3 nm in size imbedded in stoichiometric SiO_2. At fields below 2 MV/cm, trapping at these clusters explains the observed current. At higher fields the conduction is a combination of tunneling between small silicon islands and field-enhanced injection from the islands into the oxide conduction band. The threshold for this conduction is sensitive to the density and size distribution of the silicon clusters. Single implant SIMOX is thought to have a higher density of clusters and normally has a lower threshold for tunneling (20).

Note that neither the localized leakage or the low-field tunneling are produced by high annealing temperature alone. The BESOI material annealed at 1300°C has conduction that is typical of thermal oxide (18). The excess conduction in SIMOX results from the formation process in which a mixed phase of silicon and silicon precipitates coalesce to form the buried oxide.

Two methods of introducing additional oxygen into the buried oxide of SIMOX have shown improved resistivity. The methods, which are described in the preceding section, are supplemental SIMOX and ITOX. For both methods, the concentration of silicon inclusions and silicon clusters is reduced. Presumably, the introduction of extra oxygen oxidizes the excess Si in the BOX.

Charge Trapping in SIMOX and BESOI

Irradiation studies into the total dose response of SIMOX have shown that the concentration of electron and hole traps in the buried oxide is much higher than in thermally grown oxides. Boesch et al. performed pulsed irradiation experiments in which a net positive charge buildup within the buried oxide was observed within a fraction of a second after the pulse (21). The charge buildup was attributed to the emptying of electrons captured in shallow traps during the radiation pulse. Following the pulse, the electrons were thermally excited from the trap and the trap depth was determined to be 0.5 eV. Modeling suggested that the hole motion was on the order of 10 nm before being trapped. Much less hole trapping is normally observed in thermal oxides. X-ray-induced photocurrent measurements by Pennise and Boesch also indicated that nearly all holes were trapped within the buried oxide (22). The presence of deeper electron traps that retain electrons at room temperature was shown by Ouisse et al. (23). After the initial positive charge buildup due to hole trapping, there was a turnaround of the charge at the anode interface and at higher doses the net charge sensed became negative.

The high levels of electron and hole trapping in the buried oxide of SIMOX are illustrated in Figs. 2 and 3 and are compared to typical thermally grown silicon dioxide. These figures are from studies by Stahlbush et al., in which the electron and hole traps are filled by cryogenic irradiation (18,24). Electron trapping is shown in Fig. 2. Following irradiation, the cryogenic temperature was maintained and electrons were detrapped by field-induced tunneling. In the SIMOX sample, labeled Control, there is a large increase in the net positive charge, monitored by capacitance-voltage (CV) measurements, as electron traps are emptied in the field range
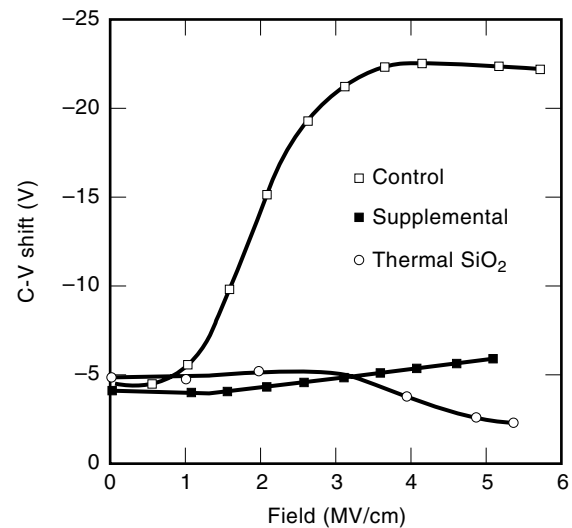

Figure 2. Comparison of electron trapping in the buried oxide of SIMOX and thermally grown silicon dioxide. The electron traps were filled by irradiation at 40 K, 100 krad (SiO_2) with grounded capacitor gates, and emptied at 40 K by field-induced tunneling. Results for normal SIMOX, labeled Control, and for SIMOX with a supplemental implant are compared to thermal SiO_2. The negative C-V shift is proportional to the net positive charge and is given with respect to its value before irradiation.

between 1 MV/cm to 3 MV/cm. In contrast, no electron trapping is observed in the thermal oxide sample. The decrease in positive charge in the 3 MV/cm to 5 MV/cm range is due to field-induced hole motion. Due to the high concentration of hole traps in SIMOX, field-induced hole motion is suppressed in the SIMOX samples. The third curve, showing results from
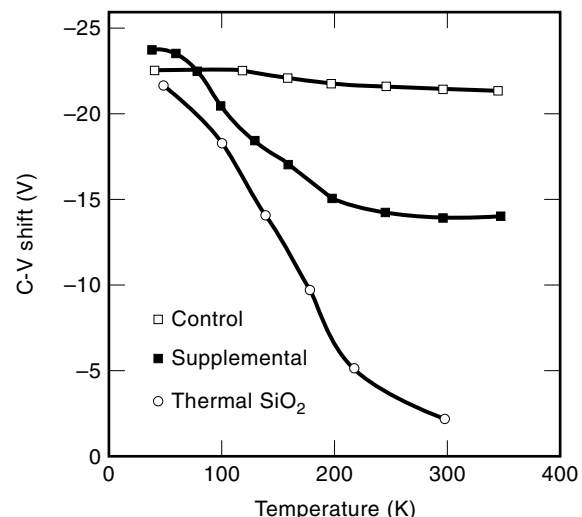

Figure 3. Comparison of hole trapping in the buried oxide of SIMOX and thermally grown silicon dioxide by isochronal annealing. Holes were generated by irradiation at 40 K. The dose for the supplemental SIMOX and thermal SiO_2 was 1 Mrad (SiO_2) with grounded gates. The dose for the normal SIMOX, labeled Control, was 100 krad (SiO_2) and was followed by electron detrapping at 40 K. At 40 K all holes are either trapped or frozen in place because they have low mobility. With annealing, holes that are not trapped become mobile and escape the oxide. The negative C-V shift is proportional to the net positive charge and is given with respect to its value before irradiation.

a supplemental SIMOX buried oxide, is discussed later. The field dependence of the electron detrapping yields a tunneling trap depth of 0.9 eV. Isochronal annealing in the same work gave the same 0.5 eV thermal trap depth as cited in the preceding. The difference between the tunneling and thermal trap depths was attributed to the polar nature of silicon dioxide and the local atomic rearrangement possible during thermal excitation but not possible during tunneling.

The high concentration of hole traps in SIMOX is illustrated in Fig. 3. Holes were captured by cryogenic irradiation. At low temperatures, hole mobility is thermally activated and goes to zero at cryogenic temperatures. Thus, all of the holes created by irradiation are held in place. The figure shows the release of the holes as the temperature is raised and the hole mobility increases. In the thermal oxide, most of the holes escape from the oxide without being trapped. In contrast, there is negligible hole motion in the SIMOX. The concentration of hole traps is high, and holes are either trapped during the irradiation or are trapped within a short distance once they become mobile. The supplemental SIMOX curve will be discussed later.

The high concentrations of electron and hole traps in the buried oxide of SIMOX have been shown to be produced by the high-temperature anneal necessary to improve the quality of the top silicon layer. A study by Stahlbush et al. has shown that the high-temperature annealing of any silicon dioxide layer encapsulated between silicon layers produces electron and hole traps (18). Buried oxides in SIMOX, ZMR and BESOI wafers were compared. The buried oxide is formed by thermal oxidation for the ZMR and BESOI technologies while the SIMOX buried oxide is formed by implantation and annealing. The SIMOX and ZMR fabrication both include high-temperature annealing above 1300°C. The normal annealing temperature to strengthen the bond in the BESOI material is 1100°C. The BESOI with and without this anneal was examined. Also included were BESOI materials annealed at 1200 and 1300°C. The 1100°C anneal increased the hole trapping in the BESOI samples (25). Even more hole trapping occurred in the SIMOX and ZMR material as well as in the BESOI annealed at the higher temperatures. Electron trapping, such as that shown in Fig. 2, also increased as the annealing temperature increased. Calculations of the thermal and tunneling trap depths show that the same types of electron traps are present in the SIMOX, ZMR, and BESOI buried oxides. Thus, buried oxides formed by very different techniques develop similar traps when given the same high-temperature anneal. The trap formation is also strongly affected by the fact that the oxide is encapsulated between silicon layers. Thermal oxides not encapsulated by silicon have significantly less electron trapping. The nonencapsulated oxides include thermal oxides grown at 1300°C as well as ones grown at lower temperature and annealed in argon at 1300°C.

From the similar charge trapping observed in any buried silicon dioxide layer, it was concluded that high-temperature annealing produces a chemically reduced oxide and that defects in the oxygen deficient SiO_2, such as Si–Si bonds, are responsible for the electron and hole trapping. Electron trapping in SIMOX can be reduced by removing the top silicon layer and annealing the oxide in oxygen at 1100°C (18,20). Additional evidence is provided by studies made by Devine et al., in which a buried oxide formed by covering the oxide by polysilicon was annealed at 1300°C (13). They observed the simultaneous increase of E′ centers near the silicon-oxide interfaces and of oxygen dissolved in the silicon. (A standard E′ center is a hole trapped at an oxygen vacancy; E′ centers are discussed in the EPR section that follows.) Note that the silicon-rich defects produced by high-temperature annealing are point defects and different from the larger silicon defects already discussed here.

The formation of electron traps has been studied in more detail over the temperature range of 1100° to 1325°C by Stahlbush and Brown (26), and Stahlbush (27). The buried oxide was formed by covering pyrogenically grown oxide with polysilicon. Two electron traps were produced. In addition to the electron trap present in SIMOX and the other buried oxides annealed near 1300°C, a deeper trap is observed. Neither trap is observed before annealing. In contrast to the more shallow trap that is not occupied at room temperature, the deeper trap is occupied by room-temperature irradiation. Trapping in the more shallow trap increases with annealing temperature while trapping in the deeper trap is maximum near the lower end of the studied annealing range. The temperature of maximum trapping depends on the buried oxide thickness. The maximum is near 1175°C for 400 nm thickness and 1100°C or lower for 100 nm thickness.

The presence of two electron traps is shown in Fig. 4. This figure displays the results of filling electron and hole traps by
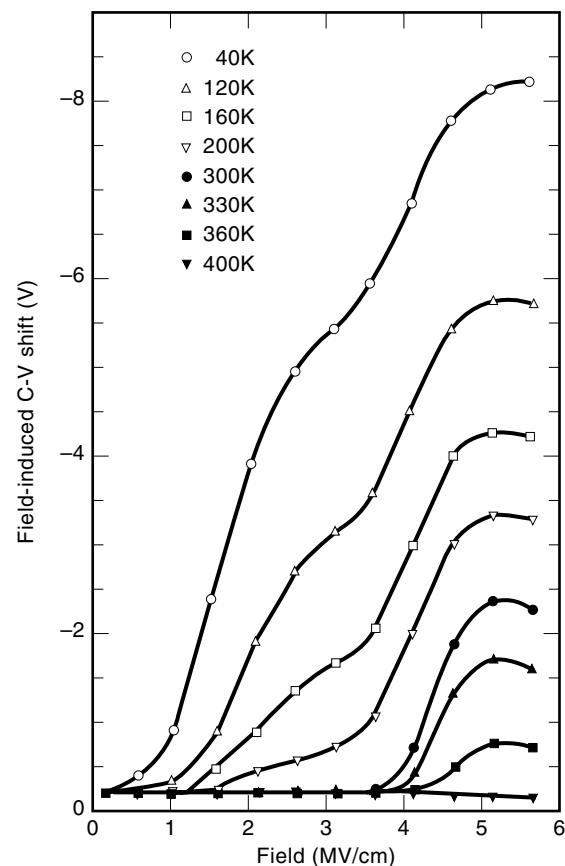

Figure 4. Electron trapping in 400 nm buried oxide covered by polysilicon and annealed at 1175°C. The electron traps were filled by irradiation at 40 K, 100 krad (SiO_2) with grounded capacitor gates. They are emptied by a two step process: (1) an isochronal anneal with gates grounded; and (2) field-induced tunneling at 40 K. Curves are shown for annealing temperatures from 40 K to 400 K. The negative C-V shift is proportional to the net positive charge and is given with respect to its value after irradiation.

irradiation at 40 K and emptying the electron traps by a two-step process. The first step is an isochronal anneal ranging from 120 K to 400 K with zero applied field. During this step, electrons that are thermally excited from traps recombine with holes. In the second step, electrons that remain in the traps are removed by field-induced tunneling and are swept from the oxide by the field. Results from a 400 nm thick buried oxide that was annealed at 1175°C are shown in the figure. Both the field and temperature dependencies demonstrate the presence of two electron traps. Electrons that are in the more shallow trap tunnel in the field range from 1 MV/cm to 3 MV/cm and are completely thermally detrapped by 300 K, room temperature. Electrons that are in the deeper electron trap tunnel in the field range from 3.5 MV/cm to 5 MV/cm. The detrapping is the same in this field range for the 40 K to 300 K curves, indicating that no thermal detrapping from the deeper traps occurs up to room temperature. By 400 K, electrons in the deeper trap are completely removed by thermal excitation. The calculated tunneling depths of the two traps are 0.9 and 1.5 eV and depths calculated for the thermal traps depths are 0.5 and 1.1 eV.

Electron traps that are deeper cannot be measured by this method. At fields of 6 MV/cm and higher, Fowler–Nordhiem injection of electrons into the oxide begin to affect both electron and hole trap occupation. Thus, electron traps that are deeper than about 2 eV can not be studied by this method. It is possible that electron traps filled by techniques such as photoinjection at room temperature do occupy traps that are 2 eV or deeper.

Studies by Devine et al., Stahlbush and Brown, and Warren et al. (13,26,28) have shown that chemical reduction of the buried oxide by annealing is a diffusion limited process that proceeds from the silicon-oxide interfaces. The details of this process are not well understood. Devine et al. (13) have suggested that network oxygen diffuses from the oxide and is dissolved into the silicon. This mechanism accounts for the oxygen increase in the silicon, but underestimates the rate of E′ center formation in the oxide. Stahlbush and Brown (26) have suggested that either SiO or CO diffuse from the silicon-oxide interfaces into the oxide and react to reduce the oxide. The formation rate of electron traps was shown to be consistent with those diffusing species. However, the results are not conclusive.

Electron trapping in SIMOX has also been studied by Afanas'ev et al. by photoinjection (20). Two types of electron traps are observed. The first type has a capture cross section greater than 10^{13} cm² and is attributed to silicon clusters that were calculated to be 1 nm to 4 nm in size. The second type of electron trap has a capture cross section on the order of 10^{14} cm² and is attributed to the point defects typical of silicon dioxide. Those SIMOX samples with lower concentrations of silicon clusters (such as triple implant SIMOX) have a lower concentration of the first type of electron trap.

Also shown in Figs. 2 and 3 is the decrease in electron and hole trapping typical of supplemental SIMOX material. In Fig. 2, electron detrapping is shown in SIMOX before and after the supplemental oxygen implant. An order of magnitude decrease of electron trapping during irradiation is attained. The decrease in hole trapping is shown in Fig. 3. As the temperature rises and the holes become mobile, some of the holes escape the buried oxide before being trapped. The amount of hole trapping shown in this figure is intermediate

between the hole trapping of thermal oxide and conventional SIMOX. Not all supplemental implant samples have as much improvement. There were variations among batches of SIMOX wafers. The best results are shown in Fig. 3. Photoinjection results also show that the electron trapping associated with point defects is decreased (20).

ELECTRON PARAMAGNETIC RESONANCE

In an attempt to understand and minimize the problems already described here, several spectroscopic studies have been undertaken. One of the most common techniques used to study point defects in SOI is electron paramagnetic resonance (EPR), a spectroscopy used to study the concentration and atomic structure of microscopic defects in materials. Identification of individual defects by EPR relies on the absorption of microwaves between energy levels produced by the interaction between an applied magnetic field and unpaired electron (Zeeman Interaction) (29). To increase sensitivity, the field is modulated and the derivative of the absorption is recorded. The magnetic field at the peak of the absorption appears where the signal intensity passes through zero and is referred to, therefore, as B_{zero}. B_{zero} is often reinterpreted as a g value through the relation $g = h\nu/[\mu_b B_{zero}]$. Here, h is Planck's constant, ν is the microwave frequency, and μ_b is the Bohr magneton. For the doublet centers to be discussed here, the g value is the average value of the two absorption lines. An EPR spectrum obtained from 10 Mrad γ-ray irradiated SIMOX is shown in Fig. 5. Annealing studies indicate that two centers are represented, E_δ' and E_γ'. Arrows point to the zero crossings from which the g value is determined. In principle, EPR spectra can be characterized by a **g**-tensor, representing the symmetry of the defect with respect to the sur-
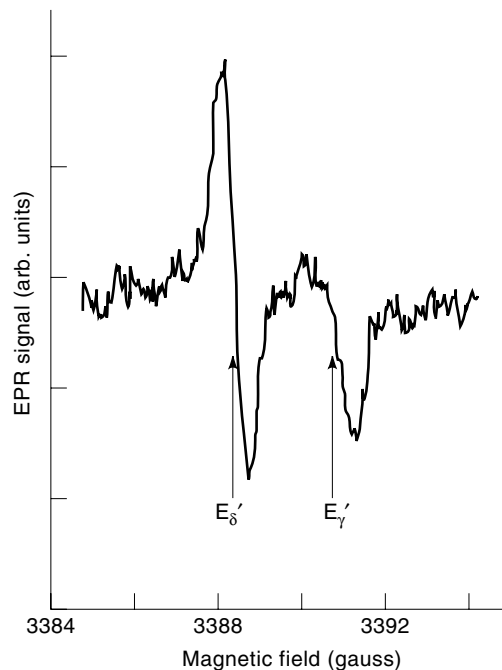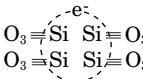
Figure 5. The EPR spectrum of 10 Mrad γ-ray irradiated standard SIMOX. The E_δ' has a zero crossing at $g = 2.0017$ and E_γ' has a zero crossing at $g = 2.0006$.

Table 1. EPR Detected Defects in Si/SiO₂/Si Structures ($O_3\equiv Si–O–Si\equiv O_3$ is the ideal structure)

EPR Center	Structural Model	SOI Type	SOI Layer	Radiation	Electrical[d] Behavior	Reference
E'_γ $g = 2.0005 - 2.0010$	$O_3\equiv Si-\ Si\equiv O_3$	both	oxide	all	positively charged	31,32
E'_δ $g = 2.0017 - 2.0021$	$O_3\equiv Si\ Si\equiv O_3$ $O_3\equiv Si\ Si\equiv O_3$	SIMOX	oxide	all[c]	positively charge	33,34,35
74 G Doublet $g = 2.0016$	$O_3\equiv Si–H$	SIMOX	oxide	all	not known	36,37
10.4 G Doublet $g = 2.0005$	$H-O_3\equiv Si-$	SIMOX	oxide	all	not known	36,37
$g = 2.0042$ $g = 2.0061$	$?\equiv Si-$	BESOI	near top interface	VUV hole injection	positively charged	32,38
EH $g = 2.0025$	E′-like, involves hydrogen	BESOI	near top interface	VUV hole injection	positively charged	32
Si Pb[a] $P_{b0}, g = 2.0060$ $P_{b1}, g = 2.0032$	$Si_3\equiv Si-\ Si\equiv O_3$	SIMOX	Si/SiO₂ interfaces	none[c]	amphoteric[e]	39,40
UL1[a] (10 K) $g = 1.99994$	(b)	both	Si	none[c]	shallow donor[e]	41,42,32

[a]Measured with the magnetic field parallel to the Si (100) direction.
[b]Many possible structures. See references.
[c]Known to be influenced by the thermal history of the sample. See text and references.
[d]See text and references for interpretation of listing.
[e]No data available for SOI. The assignment is based on the SiO₂/Si system for P_b and bulk Si for UL1.

rounding lattice, and a hyperfine tensor, representing the strength and direction of interaction of the electron with nearby nuclei. Unfortunately, the low signal-to-noise ratio inherent in spectra obtained from these thin-film samples limits the availability of these detailed data. Thus, the buried oxide absorption lines are often simply identified by B_{zero} or, equivalently, the g value. Details of the atomic structure are borrowed from studies of bulk silica (pure amorphous SiO_2) or bulk silicon.

Table 1 lists the properties of the defects identified in buried oxides by EPR. Several clarifications should be noted. First, the g values cited are derived from the zero crossings of the magnetic field. For anisotropic centers, the **g** tensor may be found in many of the references cited. Second, none of the models are derived from buried oxide EPR data. Rather, the necessary spectroscopic information used to develop the atomic structure comes from studies of bulk material or, for the P_b center, Si/SiO₂ structures. Finally, it is important to realize that EPR senses only those defects with a single unpaired electron. Thus, the *defects* (precursors) that give rise to paramagnetic *centers* could be present in the as-formed, untreated SOI wafer. The structural models represent the EPR active center, not the precursor defect. In only one case, the E'_γ center, is the precursor well-established. See Ref. 29.

The types of radiation used to activate the centers are vacuum ultraviolet (VUV), X rays, and γ rays. All forms create electron-hole pairs in the oxide. Unlike X rays and γ rays, VUV is absorbed in the top 10 nm of SiO_2, so the electron-hole pairs are created near the upper surface of the oxide. When the VUV radiation is used while an electrical bias is applied to the oxide, the process is called hole injection. Usually, low-energy ions from a corona discharge are used to create the electrical bias. The oxide is charged positively with respect to the substrate, causing electrons to drift out of the

oxide towards the nearby positive corona ions. Holes are "injected" into and drift through the oxide layer. For the VUV irradiation studies on buried oxides, one caveat must be kept in mind. Because VUV is absorbed by the 200 nm Si overlayer, the top Si must be removed. Devine and coworkers demonstrated that samples prepared using the traditional Si etchant, KOH, exhibit an order of magnitude more E'_γ centers than do samples that were not etched (30). Removing the Si layer with XeF_2 gas proved nonperturbing. Although the effect of a hydroxide potassium (KOH) etch has not been demonstrated for other radiation conditions or EPR centers, removal of Si with KOH for EPR studies of radiation-induced centers should be viewed with caution.

Important to the operation of a device utilizing a SOI wafer is the electrical response of the defect. This is indicated in the electrical behavior column of Table 1. The electrical activity of the centers is most often obtained by correlating the EPR signal with the CV curve shifts on samples subjected to identical radiation and/or thermal treatment. Establishing a meaningful correlation is a tremendous undertaking that involves studies of the depth, dose, and temperature dependence of the paramagnetic centers and the CV shifts. For example, for the oxide defects (E'_γ through EH) CV and EPR measurements made following hole injection often indicate an increase in positive charge and an increase in resonance signal intensity. Usually, the EPR centers are not observed after electron injection, but once established by hole injection, they can be annihilated by subsequent injection of electrons. The centers of Table 1 labeled "positively charged" exhibit these characteristics. However, in the cases cited in Table 1, the charge density and paramagnetic center density do not show a one-to-one correlation and their locations may not coincide. Therefore, "positively charged" is not a definitive statement. Rather, it is a working hypothesis based on the simultaneous

increase of trapped positive charge and EPR signal intensity. Presumably the lack of one-to-one correlation between oxide trapped charge and EPR defect concentration in these samples results from the many trapped electrons known to exist in buried oxides. The trapped electrons most likely compensate most of the positively charged EPR detected defects. Similar to the situation in bulk silica, the defects in SOI associated with the trapped electrons do not appear to be EPR active. The charge state of the two Si-based centers in the table have not been studied in SOI. The assignments listed are borrowed from the Si/SiO$_2$ system or bulk Si.

An article by Warren et al. conveniently summarizes the properties of most of the centers listed in Table 1 (32), so there is no need to detail the results here. The following covers work done since publication of the Warren publication, and discusses a few centers not presented in that article.

There has been much activity recently in the study of the E$'_\delta$ center in both thin film and bulk SiO$_2$. Based on hyperfine data in pure bulk silica, Zhang and Leisure (33) modified the five-Si cluster model originally proposed by Vanheusden and Stesmans (35). As depicted in Table 1, the Zhang model for E$'_\delta$ eliminates one Si from the cluster. However, this does not alter most of the conclusions made concerning the E$'_\delta$ center in BOX: in particular, that the center is likely to be positively charged when paramagnetic remains valid (32). As noted in Table 1 but not in the Warren article, E$'_\delta$ may be generated by X rays or γ rays, but the net generation rate is substantially smaller than that found using hole injection. Further, relatively low doses must be used because the E$'_\delta$ center saturates at about 3 Mrad, and beyond that dose it is easily overwhelmed by the E$'_\gamma$ center (33,43). Since publication of the Warren article, the E$'_\delta$ density has been shown to correlate with the thermal history of the sample. A study using polysilicon-coated thermal oxides heat treated between 700°C and 1325°C demonstrated that temperatures of 1000°C are required to observe the E$'_\delta$ center and that the density does not change between 1000°C and 1325°C (43). Further, heat treatment in both an inert ambient and an oxidizing ambient produce approximately the same density of centers.

A second center briefly discussed in the Warren article is the Si dangling bond or D center, a defect in crushed Si or a-Si. Table 1 entries, $g = 2.0041$ and $g = 2.0061$, refer to this center. As alluded to in the article by Warren et al. (32), the center most likely is a variation of the D center in which one or more Si atoms is replaced by an oxygen atom. Many combinations are possible and have been observed in both bulk and nonburied thin film SiO$_2$ (32,38,44). It is important to realize that the centers at $g = 2.0041$ and $g = 2.0061$ are not located in the bulk Si. Rather they are found in a Si-rich oxide layer or oxygen-rich Si layer.

One of the few omnipresent impurities that persists in microelectronic grade materials is hydrogen. Although SIMOX oxides are analogous to dry oxides, both SIMOX oxides and the buried oxide of BESOI wafers contain defects thought to be associated with hydrogen. The EPR spectra for each type of defect are shown in Figs. 6 and 7. Figure 6 depicts the 74G doublet observed in SIMOX after 210 Mrad γ-ray irradiation (6a) or 40 h VUV irradiation (6b). The 74G doublet was first attributed to the hydrogen-related E$'$ center by Vitko (36), and was studied in SIMOX by Conley and Lenahan (37). The name refers to the magnetic field separation between the two low intensity absorption lines situated on each side of the central E$'$ line at $g = 2.0005$. The central line represents a non-
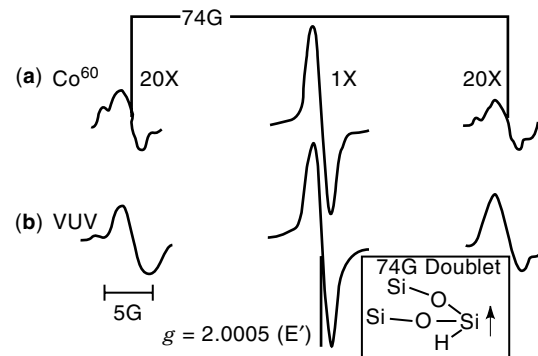

Figure 6. EPR spectra of the 74 G doublet in SIMOX buried oxides generated by (a) Co^{60} and (b) VUV irradiation. The central resonance is due to the standard E$'$ center. The side resonance separated by 74 G represents the interaction of the E$'$ center with a nearby hydrogen. The insert shows the proposed atomic structure of the defect responsible for the 74 G doublet. (Reprinted with permission from "Room temperature reactions involving Si dangling bond centers and molecular hydrogen in amorphous SiO$_2$ thin films in Si", J. F. Conley and P. M. Lenahan, *IEEE Trans. Nucl. Sci.,* **39**: 2186, 1992. © 1992 IEEE.)

hydrogen associated E$'$ center listed in Table 1. In the same material, a similar center with hyperfine splitting of 10.4 G is also observed. Conley and Lenahan show that in SIMOX both doublets increase with 110°C forming gas treatment, while the central E$'$ line decreases. The numerical agreement between the E$'$ decrease and doublet increase implies a direct correlation between the hydrogen-related and nonhydrogenated E$'$ centers. Significant to electronic films, the work suggests that hydrogen migrates to the standard E$'$ centers on time scales of minutes at temperatures as low as 100°C. Because of the similarity between these kinetics and those found for electrically active defects located at the Si/SiO$_2$ interface (interface states), the results indicate that E$'$ centers could play an active role in interface state generation.

Figure 7 was obtained on a BESOI wafer before (a) and after (b) VUV radiation, and illustrates that VUV radiation
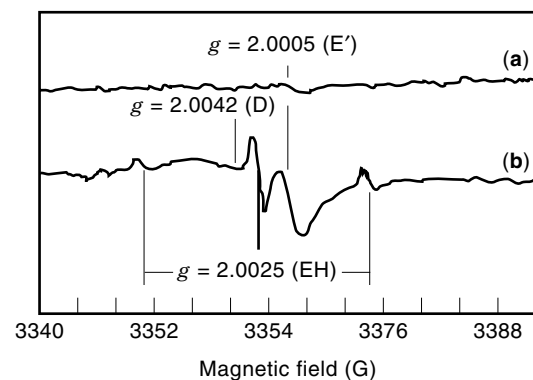

Figure 7. The EPR spectra of BESOI buried oxides (a) before and (b) after VUV illumination. The two side resonances labeled $g = 2.0025$ (EH) are separated by 23.1 G and are thought to arise from the interaction of a Si dangling bond with hydrogen. (Reprinted with permission from "Hydrogen interaction with delocalized spin centers in buried SiO$_2$ thin films", W. L. Warren, J. R. Schwank, M. R. Shaneyfelt, D. M. Fleetwood, and P. S. Winokur, *Appl. Phys. Lett.,* **62**: 1661, 1993. Copyright 1993 American Institute of Physics.)

can produce the EH center (32). The EH center, which has no known analog in bulk silica, is identified by the 23.1G hyperfine splitting centered about a central line $g = 2.0025$. Of the several common impurities in Si that could yield a two-line hyperfine spectrum, it is argued that only hydrogen could account for all of the observed data. A structural model of the center does not yet exist, but several properties pertinent to electronic device operation are reported. The center is unstable at room temperature, is generated by hole injection and, most significantly, is located near the interface between the top Si layer and the buried oxide. Because of the location just below the device active Si layer, this defect may play a role in the leakage currents that often plague devices built on buried oxide layers (32).

Several centers, E'_δ, E'_γ, and UL1 listed in Table 1, have recently been studied in SIMOX wafers that received a post-fabrication O implantation and anneal (45). In these supplemental SIMOX samples, the second O implant dose was about one-tenth the total dose for SIMOX fabrication and the post-supplemental implant anneal was performed at 1100°C for 1 h. The EPR study included several variations of SIMOX subjected to different annealing conditions. The overall results show that the supplemental O implant reduces the densities of the oxygen deficient E'_δ and E'_γ centers by a factor of 5 and 3, respectively. Consistently, the concentration of the UL1 center, the O related donor in the silicon, is increased by the supplemental oxygen dose. Clearly, the additional implantation is reaching the oxide layer and "filling the gaps"; however, the straggle in the implant profile leaves the top silicon layer afflicted with increased oxygen. Despite this, electrical measurements show that the supplemental implantation improves oxide resistivity (see the "Electrical Characterization" section of this article).

The EPR measurements on SIMOX indicate that a 550°C forming gas (H_2:N_2 mixture) or N_2 treatment generates P_b centers, Si dangling bonds located on the Si side of a Si/SiO_2 interface. Earlier investigators observed P_b centers in unannealed SIMOX and attributed their presence to oxide precipitates known to exist in unannealed oxygen implanted Si. The most recent work reports P_b centers in fully annealed SIMOX and attributes their presence to the Si/SiO_2 interfaces (40). The density of centers in the buried oxide is twice that in nonburied oxides subjected to identical treatments. The factor of two suggests that the difference between nonburied and buried oxides reflects the dual Si/SiO_2 interfaces of the latter. However, the "two" may be coincidental, and the larger number of interface centers may result simply from the greater degree of dryness offered by the moisture impervious top Si layer covering the buried oxides. (The correlation between P_b centers and hydrogen species such as moisture has been well-established by other researchers.) The study of P_b centers in SIMOX also notes that the electrically measured interface state density is numerically similar to the density of P_b centers. The correlation suggests that the density of states at the interface is due largely to the interfacial Si dangling bonds. Recently, Vanheusden et al. reported a second consequence of forming gas anneals, the formation of positive charge and mobile protons (46).

SUMMARY AND FUTURE TRENDS

For successful commercialization of this technology, SOI must meet two requirements: (1) the top Si layer must be uniform and be as defect free as bulk Si wafers; and (2) the buried oxide must provide good isolation without compromising the operation of the devices in the top layer. Uniformity is now only slightly less than Si for all SOI processes; however, residual defects in the surface Si remain a concern. The buried oxide quality is more of a concern in SIMOX than in bonded wafers. The BOX of both, however, appears to deteriorate after the extended high temperature anneal required to produce a useful Si layer for SIMOX or strengthen the bond in BSOI. Nevertheless, both technologies have produced successful devices. More importantly, new markets for SOI are emerging. The largest potential market is for low-power integrated circuits. The inherent ability of SOI to operate at high speed and low voltage makes it an attractive technology for low-power applications and is driving efforts to improve SOI wafers.

BIBLIOGRAPHY

1. B. El-Kareh, B. Chen, and T. Stanley, Silicon on insulator—an emerging high-leverage technology, *IEEE Trans. Compon. Packag. Manuf. Technol. A,* **18** (1): 187–194, 1995.

2. P. L. F. Hemment, Silicon on insulator formed by O+ or N+ ion implantation, *Mat. Res. Soc. Symp. Proc.,* **53**: 207–220, 1986.

3. J. Stoemenos, Silicon on insulator obtained by high dose oxygen implantation, microstructure, and formation mechanism, *J. Electrochem. Soc.,* **142** (4): 1248–1260, 1995.

4. M. A. Mendicino et al., A comparative evaluation of 200 mm SOI wafers through state-of-the-art materials characterization, in P. L. F. Hemment et al. (eds.) *Silicon-on-Insulator Technology and Devices,* The Electrochemical Society, Inc., **96-3**: 148, 1996.

5. S. Nakashima et al., Investigations on high-temperature thermal oxidation process at top and bottom interfaces of top silicon of SIMOX wafers, *J. Electrochem. Soc.,* **143** (1): 244–251, 1996.

6. M. Tachimori et al., Quality innovation of SIMOX wafers by low-dose and high-temperature oxidation techniques, in *Silicon-on-Insulator Technology and Devices* P. L. F. Hemment et al. (eds.), The Electrochemical Society, Inc. **96-3**: 53, 1996.

7. O. W. Holland, D. Fathy, and D. K. Sadana, Formation of ultrathin, buried oxides in Si by O$^+$ ion implantation, **69**: 674, 1996.

8. C. Harendt et al., Silicon on insulator material by wafer bonding, *J. Electron. Mater.,* **20** (3): 267–277, 1991.

9. W. P. Maszara, Silicon-On-Insulator by wafer bonding: A review, *J. Electrochem. Soc.,* **138** (1): 341–347, 1991.

10. C. Maleville et al., Physical phenomena involved in the Smart-Cut process, in *Silicon-on-Insulator Technology and Devices* P. L. F. Hemment et al. (eds.), The Electrochemical Society, Inc., **96-3**: 34, 1996.

11. S. Nakashima and K. Izumi, Buried oxide layers formed by low-dose oxygen implantation, *J. Mater. Res.,* **7**: 788, 1992.

12. S. Nakashima and K. Izumi, Analysis of buried oxide layer formation and mechanism of threading dislocation generation in the substoichiometric oxygen dose region, *J. Mater. Res.,* **8** (3): 523–534, 1993.

13. R. A. B. Devine et al., Oxygen gettering and oxide degradation during annealing of Si/SiO_2/Si structures, *J. Appl. Phys.,* **77**: 175, 1995.

14. Y. Li et al., Oxygen isotopic exchange during the annealing of low energy SIMOX layers, *Nucl. Instrum. Methods Phys. Res. B,* **85**: 236–242, 1994.

15. G. A. Brown and A. G. Revesz, Defect electrical conduction in SIMOX buried oxides, *IEEE Trans. Electron Devices,* **ED-40**: 17000, 1993.

16. K. Joyner, M. El-Ghor, and H. Hosack, Effects of particles on the buried oxide defects in SIMOX material, *IEEE/SOI Conf. Proc.,* 1991, p. 4.

17. A. G. Revesz, G. A. Brown, and H. L. Hughes, Bulk electrical conduction in the buried oxide of SIMOX structures, *J. Electrochem. Soc.,* **140**: 3222, 1993.

18. R. E. Stahlbush et al., Electron and hole trapping in irradiated SIMOX, ZMR and BESOI buried oxides, *IEEE Trans. Nucl. Sci.,* **NS-42**: 2086, 1992.

19. D. J. DiMaria et al., Charge transport and trapping phenomena in off-stoichiometric silicon dioxide films, *J. Appl. Phys.,* **54**: 5801, 1983.

20. V. V. Afanas'ev, A.G. Revesz, and H. L. Hughes, Confinement phenomena in buried oxides of SIMOX structures as affected by processing, *J. Electrochem. Soc.,* **143**: 695, 1996.

21. H. E. Boesch et al., Time dependent hole and electron trapping effects in SIMOX buried oxides, *IEEE Trans. Nucl. Sci.,* **NS-37**: 1982, 1990.

22. C. A. Pennise and H. E. Boesch, Jr., Determination of the charge-trapping characteristics of buried oxides using a 10-keV X-ray source, *IEEE Trans. Nucl. Sci.,* **NS-37**: 1990, 1990.

23. T. Ouisse, S. Cristoloveanu, and G. Borel, Electron trapping in irradiated SIMOX buried oxides, *IEEE Trans. Electron Devices Lett.,* **12**: 312, 1991.

24. R. E. Stahlbush, H. L. Hughes, and W. A. Krull, Reduction of charge trapping and electron tunneling in SIMOX by supplemental implantation of oxygen, *IEEE Trans. Nucl. Sci.,* **NS-40**: 1740, 1993.

25. J. B. McKitterick, A. Caviglia, and W. P. Maszara, Total dose hardness of bonded SOI wafers, *IEEE Trans. Nucl. Sci.,* **NS-39**: 2098, 1992.

26. R. E. Stahlbush and G. A. Brown, Bulk trap formation by high temperature annealing of buried thermal oxides, *IEEE Trans. Nucl. Sci.,* **NS-42**: 1708, 1995.

27. R. E. Stahlbush, Electron trapping in buried oxides during irradiation at 40 and 300 K, *IEEE Trans. Nucl. Sci.,* **NS-43**: 1996.

28. W. L. Warren et al., Microscopic nature of border traps in MOS oxides, *IEEE Trans. Nucl. Sci.,* **NS-41**: 1817, 1994.

29. W. Gordy, in W. West (ed.) *Techniques of Chemistry,* Vol. 15: New York: Wiley, 1980.

30. J. L. Leray, J. Margail , and R. A. B. Devine, Electric field dependent paramagnetic defect creation in single step implanted SIMOX films, *Mater. Sci. and Eng.,* **B12:** 153, 1992.

31. D. L. Griscom, Characterization of 3 E′ variants in X- and γ-irradiated high purity a-SiO$_2$, *Nucl. Instrum. Methods Phys. Res. B,* **1**: 481–488, 1984.

32. W. L. Warren et al., Paramagnetic defect centers in BESOI and SIMOX buried oxides, *IEEE Trans. Nucl. Sci.,* **40**: 1755, 1993.

33. L. Zhang and R. G. Leisure, The E$'_\delta$ and triplet-state centers in x-irradiated high-purity amorphous SiO$_2$, *J. Appl. Phys.* **80**: 3744, 1996.

34. A. Stesmans and K. Vanheusden, Generation of delocalized E$'_\delta$ defects in buried Si oxide by hole injection, *J. Appl. Phys.,* **76**: 1681, 1994.

35. K. Vanheusden and A. Stesmans, Characterization and depth profiling of E′ defects in buried SiO$_2$, *J. Appl. Phys.,* **74**: 275, 1993.

36. T. E. Tsai and D. L. Griscom, On the structures of hydrogen-associated defect centers in irradiated high-purity a-SiO$_2$:OH, *J. Non-Cryst. Solids,* **91**: 170–179, 1987.

37. J. F. Conley and P. M. Lenahan, Room temperature reactions involving Si dangling bond centers and molecular hydrogen in amorphous SiO$_2$ thin films in Si, *IEEE Trans. Nucl. Sci.,* **39**: 2186, 1992.

38. T. Inokuma et al., Electron spin resonance spectra of silicon dangling bonds with oxygen back bonds in plasma-deposited amorphous SiO$_x$, *J. Electrochem. Soc.,* **142** (7): 2346–2351, 1995.

39. E. H. Poindexter et al., Electronic traps and P$_b$ centers at the Si/SiO$_2$ Interface: Band-gap energy distribution, *J. Appl. Phys.,* **56**: 2844, 1984.

40. K. Vanheusden et al., Nonuniform oxide charge and paramagnetic interface traps in high-temperature annealed Si/SiO$_2$/Si structures, *Appl. Phys. Lett.,* **68**: 2117, 1996.

41. W. L. Warren et al., Shallow oxygen-related donors in bonded and etchback silicon on insulator structures, *Appl. Phys. Lett.,* **64**: 508, 1994.

42. P. Wagner et al., in P. Grosse (ed.) *Festkorperprobleme (Advances in Solid State Physics),* Vol. 24, Braunschweig: Vieweg, 1984, p. 191.

43. M. E. Zvanut and T. L. Chen, Production of E$'_\delta$ center induced by dry heat treatment of non-buried SiO$_2$ films, *Appl. Phys. Lett.,* **69**: 28, 1996.

44. A. Stesmans and V. V. Afanas'ev, Annealing induced degradation of thermal SiO$_2$: S center generation, *Appl. Phys. Lett.* **69**: 2056, 1996.

45. K. Vanheusden and A. Stesmans, Impact of supplemental implantation of oxygen on defect centers in the separation by implantation of oxygen structure, *Appl. Phys. Lett.,* **67**: 1399, 1995.

46. K. vanHeusden et al., Non-volatile memory device based on mobile protons in SiO$_2$ thin films, *Nature,* **386**: 587, 1997.

M. E. Zvanut
University of Alabama at
   Birmingham
R. E. Stahlbush
Naval Research Laboratory

SEMICONDUCTOR LASER PACKAGING. See Packaging of optical components and systems.

SEMICONDUCTOR LASERS, SINGLE FREQUENCY. See Distributed feedback lasers.

SEMICONDUCTOR LIGHT SOURCES. See Light-emitting diodes.

SEMICONDUCTOR MANUFACTURING. See Diagnosis of semiconductor processes; Flexible semiconductor manufacturing; Fuzzy logic for semiconductor manufacturing; Lithography; Statistical methods for semiconductor manufacturing.